ASIAN JOURNAL OF FORESTRY
Volume 9, Number 1, June 2025
Pages: 115-123

E-ISSN: 2580-2844
DOI: 10.13057/asianjfor/r090112

Estimating forest above ground biomass in Dak Lak Province, Vietnam

HO DINH BAO, NGUYEN THI THANH HUONG♥
Faculty of Agriculture and Forestry, Tay Nguyen University. 567 Le Duan St., Buon Ma Thuot City, Dak Lak, Vietnam.
Tel.: +84-914-141188, ♥email: huongthanh.frem@ttn.edu.vn

Manuscript received: 23 December 2024. Revision accepted: 17 March 2025.

Abstract. *Bao HD, Huong NTT. 2025. Estimating forest above ground biomass in Dak Lak Province, Vietnam. Asian J For 9: 115-123.* Accurately estimating forest Above Ground Biomass (AGB) is essential for assessing carbon stocks, monitoring forest health, and guiding sustainable management practices. This study examined the potential of Landsat 8 satellite imagery for AGB estimation in Dak Lak Province, located in Vietnam's Central Highlands. Field data collected from 415 sample plots across diverse forest types including evergreen broadleaf, semi-deciduous, and dry dipterocarp forests revealed AGB values ranging from 15.16 to 299.33 tons/ha. Multivariate linear regression (MLR) and random forest (RF) models were applied to predict AGB using spectral bands and vegetation indices derived from Landsat 8 imagery. The MLR model demonstrated limited predictive capability ($R^2 = 0.131$), indicating that linear relationships between spectral data and AGB were insufficient to capture the system's complexity. In contrast, the RF model exhibited superior predictive performance, achieving an R^2 of 0.653 and a concordance R^2 of 0.571 when using spectral bands alone. Incorporating vegetation indices alongside spectral bands further improved the RF model's accuracy ($R^2 = 0.671$, concordance $R^2 = 0.586$). Spatial analysis revealed considerable variability in AGB across forest types, with evergreen broadleaf forests exhibiting the highest biomass values. These findings highlight the effectiveness of satellite remote sensing and machine learning for cost-effective biomass estimation. Moreover, they highlight the urgent need for such approaches in forest management and climate change mitigation efforts in tropical regions, including Vietnam.

Keywords: Carbon stock, google earth engine, Landsat 8, linear regression, random forest

INTRODUCTION

Forest ecosystems serve as the primary terrestrial carbon reservoirs, storing approximately 80% of the biosphere's carbon and playing a crucial role in climate change mitigation (Duchelle et al. 2018). Forest biomass is a key metric for assessing carbon sequestration and the overall carbon balance of ecosystems. Accurate estimation of forest biomass is essential for understanding the carbon cycle across large terrestrial landscapes (Li et al. 2015). Forest Above Ground Biomass (AGB) is traditionally assessed through either field measurements (West 2015) or remote sensing techniques (Yang et al. 2020). While field-based methods provide the most precise AGB estimates, their large-scale application is constrained by high costs, labor intensity, and time requirements. Estimating AGB over extensive areas using traditional methods is impractical due to the need for frequent updates to capture real-time biomass values. To address these challenges, remote sensing has emerged as a powerful tool for AGB estimation, enabling the development of regional and national biomass maps (Xiao et al. 2019; Tian et al. 2023; Sa et al. 2024).

The use of remote sensing for AGB estimation has gained prominence across various ecosystems globally, with previous studies demonstrating its effectiveness in biomass assessment and monitoring. A range of remote sensing technologies, including passive and active sensors, have been applied to estimate AGB (Deng et al. 2014; Cao et al. 2016; Shen et al. 2016; Sa et al. 2024). Among available satellite platforms, Landsat 8 offers several advantages for biomass estimation, including free access to time-series data, high spatial and temporal resolution, and consistent radiometric quality (Li et al. 2020; Nguyen et al. 2020). Vegetation indices derived from Landsat spectral bands such as the Normalized Difference Vegetation Index (NDVI), Leaf Area Index (LAI), Moisture Stress Index (MSI), and Enhanced Vegetation Index (EVI) are widely employed to enhance biomass estimation accuracy (Zhang et al. 2019).

Selecting an appropriate modeling approach is essential for reliable AGB estimation. Traditional statistical models, particularly Linear Regression (LR), have been extensively applied in biomass studies (Li et al. 2019). However, classical regression techniques often fail to capture the complex, nonlinear relationships between AGB and remote sensing variables (Zhao et al. 2018). To overcome this limitation, machine learning algorithms such as decision trees, K-Nearest Neighbors (KNN), Artificial Neural Networks (ANN), and Support Vector Machines (SVM)—are increasingly used for biomass estimation (Gao et al. 2018; Liu et al. 2018). Decision-tree-based models, particularly Random Forest (RF) and Gradient Boosting (GB), have demonstrated superior predictive accuracy in biomass modeling (Belgiu and Drăgu 2016; Zhang et al. 2019; Hu and Sun 2022; Tian et al. 2024). Additionally, machine learning algorithms involve numerous adjustable parameters that significantly influence model performance, highlighting the importance of parameter tuning in optimizing predictive accuracy (Freeman et al. 2016; Probst and Boulesteix 2018).

Given the urgent need for efficient, large-scale monitoring of forest biomass, satellite remote sensing remains a cornerstone of forest management and carbon stock assessment strategies (Camarretta et al. 2023). Since the launch of the Landsat mission in the 1970s, remote sensing has played a pivotal role in forest monitoring and mapping. Among machine learning approaches, the Random Forest algorithm has gained prominence due to its high accuracy, computational efficiency, and robustness against noise and overfitting (Wang et al. 2016; Gao et al. 2018; Tian et al. 2024). Numerous studies have employed RF for satellite-based biomass estimation, demonstrating its effectiveness for large datasets.

This study evaluates the utility of Landsat 8 imagery in predicting forest aboveground biomass using the RF algorithm. The objectives were to (i) model the relationship between field-measured AGB and Landsat reflectance; (ii) compare the predictive performance of the RF model with Multiple Linear Regression; and (iii) identify the most suitable model for AGB estimation in the study area.

MATERIALS AND METHODS

Study area

Dak Lak Province is situated in the Central Highlands of Vietnam, spanning approximately 13,085 km², which constitutes 3.9% of the country's total land area. The province lies between 107°28'57" to 108°59'37" E longitude and 12°09'45" to 13°25'06" N latitude (Figure 1). The terrain is predominantly mountainous, with elevations ranging from 400 to 2,442 meters above sea level, the highest point being Chu Yang Sin Mountain. A relatively flat highland region, covering about 50% of the province, extends across its central portion. Dak Lak experiences a distinct seasonal climate, with a rainy season from May to October, driven by prevailing southwest winds. Peak rainfall occurs in July, August, and September, contributing 80-90% of the annual total. In the eastern region, influenced by the Eastern Truong Son Range, the rainy season extends until November, while the dry season lasts from November to April of the following year. The province encompasses a total natural area of 1,312,537 hectares. According to the Provincial Forest Protection Department, as of late 2022, forested land covered 497,018 hectares, including 413,845 hectares of natural forests and 83,173 hectares of plantations, resulting in a forest coverage rate of 38.03%.

Materials

Satellite data

This study utilized Landsat 8 satellite imagery, selected based on its temporal correlation with forest inventory data. Landsat 8 was launched on 11 February 2013 from Vandenberg Air Force Base, California, and is equipped with two scientific instruments: the Operational Land Imager (OLI) and the Thermal Infrared Sensor (TIRS). These instruments provide seasonal imagery of Earth's surface at spatial resolutions of 30 m (visible, near-infrared, and shortwave infrared), 100 m (thermal infrared), and 15 m (panchromatic band). Landsat 8 was developed through a collaboration between the United States Geological Survey (USGS 2023) and NASA. The OLI represents a significant technological advancement over previous Landsat sensors, incorporating innovations demonstrated by NASA's EO-1 test satellite. It features a quad-mirror telescope and 12-bit quantization, enhancing image quality and data accuracy. Additionally, the OLI includes two new spectral bands-one designed for detecting thin clouds and another for coastal observations (NASA 2024).

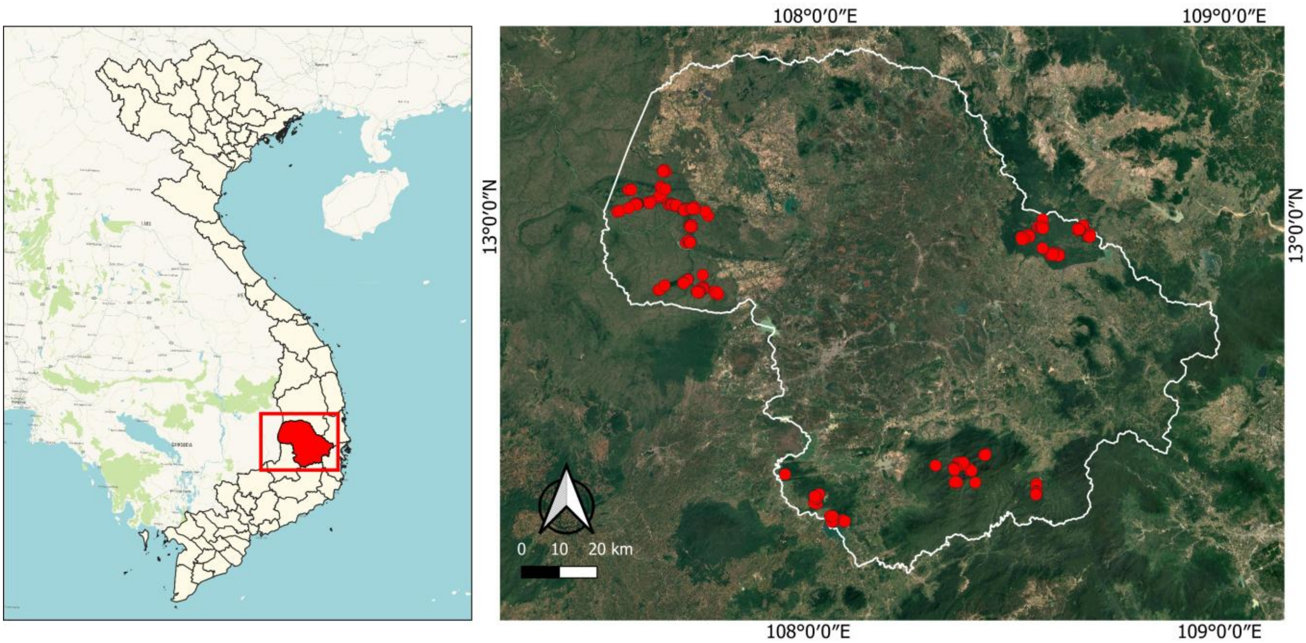

Figure 1. Location of the study area and ground plots at sites in Dak Lak Province, Central Highlands of Vietnam

Field data

Forest data for this study were collected from various natural forest types in Dak Lak Province, including dry deciduous forests, semi-deciduous forests, and evergreen broadleaf forests. Sampling was conducted using 30 × 30 m (900 m^2) plots. Within each plot, tree parameters such as height, diameter at breast height, and species composition were recorded. Above Ground Biomass (AGB) for each tree was estimated using biometric equations developed by Bao et al. (2012), specifically calibrated for natural forests in the study area. Plot-level AGB values were then obtained by summing the individual tree biomass estimates.

Methods

Satellite image processing

Landsat 8 images, pre-calibrated for atmospheric conditions and free of cloud interference, were obtained from the Google Earth Engine (GEE) platform. Vegetation indices, which characterize plant spectral properties, were derived based on strong chlorophyll absorption at 0.65 µm, using a combination of infrared and near-infrared bands. Mathematical transformations, either linear or nonlinear, were applied to multiband reflectance data to enhance vegetation-related information while minimizing interference from non-vegetation elements. This approach effectively captured vegetation conditions (Hao et al. 2024).

All primary spectral bands and derived vegetation indices were extracted and aligned with field sample plots, enabling integration with statistical analyses. Seven vegetation indices were computed to support the study: Normalized Difference Vegetation Index (NDVI) = Measures vegetation health; Enhanced Vegetation Index (EVI) = Reduces atmospheric influences for improved vegetation monitoring; Soil-Adjusted Vegetation Index (SAVI) = Adjusts for soil brightness to enhance vegetation signals; Green Normalized Difference Vegetation Index (GNDVI) = Reflects vegetation health by assessing chlorophyll concentration; Moisture Stress Index (MSI) = Estimates vegetation water content; Red Edge NDVI (RENDVI) = Utilizes red-edge spectral bands to refine NDVI measurements; Simple Ratio (SR) = Computes the ratio between near-infrared and red spectral bands.

The coordinates of sample plot centers were used to extract satellite-derived predictor variables, including spectral and vegetation indices. These variables, along with Above Ground Biomass (AGB) estimates from field data, were processed using GEE's sample raster value tool. A stratified approach was applied, allocating 80% of the dataset for model training, while the remaining 20% was reserved for accuracy assessment (Ouchra et al. 2023).

Correlation analysis

To develop a forest Above Ground Biomass (AGB) estimation model, Multiple Linear Regression (MLR) was employed for regression analysis. MLR assumes a linear relationship between the dependent variable (AGB) and a set of independent predictor variables derived from remote sensing data (Wang et al. 2015). Initially, the correlation between AGB and each spectral band and vegetation index was analyzed, and only variables exhibiting a significant correlation with AGB were selected for further analysis. Stepwise linear regression, implemented in RStudio, was used to establish the relationship between observed AGB and predictor variables extracted from Landsat imagery.

In addition to MLR, the Random Forest (RF) algorithm, a robust machine learning technique, was applied for AGB estimation. RF is widely used for both classification and regression tasks due to its ability to handle large datasets efficiently and assess the relative importance of predictor variables (Blackard et al. 2008; Belgiu and Drăgu 2016). The algorithm extends conventional decision tree models by aggregating multiple decision trees, thereby enhancing predictive accuracy and robustness against outliers (Carreiras et al. 2012). In this study, the bagging (bootstrap aggregating) algorithm was employed to generate multiple subsets of the training dataset, known as bootstrap datasets, from which decision trees were constructed and subsequently combined to form the RF model. Typically, 70% of the training samples were included in the bootstrap datasets (in-bag data), while the remaining 30% (out-of-bag or OOB data) were used for model validation. All analyses were performed using RStudio and the Google Earth Engine (GEE) platform.

Model performance was evaluated using the coefficient of determination (R^2), which measures the proportion of variance in AGB explained by the model, with higher values indicating better model performance. Additionally, the Root Mean Square Error (RMSE) was used to assess the standard deviation of residuals, where lower values indicate higher model accuracy. These metrics were used to compare the accuracy of the MLR and RF models in estimating AGB.

RESULTS AND DISCUSSION

Above ground biomass field data

A total of 415 sample plots were surveyed to collect essential forest parameters, including diameter at breast height and tree height. These parameters were used to calculate AGB for each plot, which was then converted into tons per hectare. The estimated AGB values ranged from a minimum of 15.16 tons/ha to a maximum of 299.33 tons/ha, with an average value of 96.95 tons/ha.

When analyzed by forest type, 54 plots classified as broadleaf evergreen forests exhibited AGB values ranging from 19.33 to 299.33 tons/ha. Similarly, semi-deciduous forests displayed a minimum AGB of 19.33 tons/ha. However, dry dipterocarp forests recorded a lower minimum AGB value of 15.56 tons/ha. The distribution of AGB values across different forest types is illustrated in Figure 2.

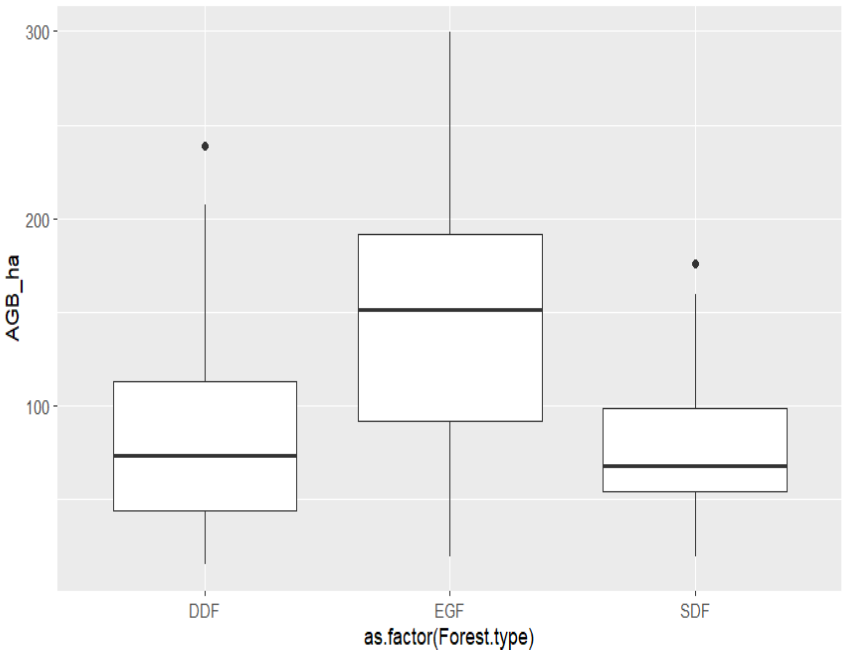

Figure 2. Distribution of calculated AGB values from survey data across different forest types. DDF = Dry Deciduous Forests; EGF = Evergreen Broadleaf Forests; SDF = Semi-Deciduous Forests

```
Coefficients:
            Estimate Std. Error t value Pr(>|t|)
(Intercept)  16.4357     2.0244   8.119 5.57e-15 ***
b4           35.6421    24.7990   1.437  0.15141
b5            0.4355    10.1106   0.043  0.96566
b6          -74.2318    24.6767  -3.008  0.00279 **
b7           17.1850    26.9139   0.639  0.52349
---
Signif. codes:  0 '***' 0.001 '**' 0.01 '*' 0.05 '.' 0.1 ' ' 1

Residual standard error: 4.852 on 410 degrees of freedom
Multiple R-squared:  0.131,     Adjusted R-squared:  0.1226
F-statistic: 15.46 on 4 and 410 DF,  p-value: 8.717e-12
```

A

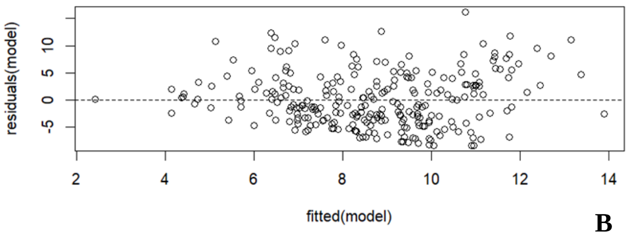

B

Figure 3. Results: A. Linear regression output summary; B. Residuals vs fitted values plot

Relationship between AGB and Landsat 8 data

Multiple linear regression analysis

A Multiple Linear Regression (MLR) model was applied to predict Above Ground Biomass (AGB) using Landsat 8 spectral bands. The model identified relationships between AGB and four spectral bands: Band 4, Band 5, Band 6, and Band 7. While the intercept (16.44, $p < 0.001$) indicated a significant baseline level of AGB, the p-values for Band 4, Band 5, and Band 7 (0.151, 0.966, and 0.523, respectively) suggested that these bands did not have statistically significant effects on AGB at the 0.05 level.

Interestingly, Band 6 exhibited a statistically significant negative coefficient (-74.23, $p = 0.003$), indicating a negative relationship between Band 6 and AGB. However, the overall explanatory power of the model was limited, with an R^2 value of only 0.131. This suggests that additional predictor variables, interactions between spectral bands, or environmental factors should be incorporated to enhance prediction accuracy. Figure 3 illustrates the regression analysis results and the residual patterns.

Random forest regression model using spectral data

The performance of the Random Forest (RF) regression model for estimating Above Ground Biomass (AGB) using Landsat spectral bands was evaluated across different numbers of decision trees (ntree). Results indicated a consistent improvement in model accuracy with increasing ntree values. For ntree = 100, the model achieved an R^2 of 0.647, and the concordance between estimated and actual AGB was strong, with a concordance R^2 of 0.549.

Increasing ntree to 200 slightly improved the R^2 to 0.650, with a concordance R^2 of 0.557. Further increases to ntree = 500 and 1000 resulted in marginal gains, with R^2 values of 0.652 and 0.653, respectively, and concordance R^2 values improving to 0.569 and 0.571. These results suggest that while increasing ntree enhances the model's ability to capture the relationship between spectral data and AGB, the improvements plateau beyond 500 trees, indicating diminishing returns. Figure 4 illustrates the concordance between actual and estimated AGB for different ntree values.

Random forest regression model using vegetation indices

The performance of the Random Forest (RF) regression model in estimating Above Ground Biomass (AGB) using vegetation indices was assessed across varying numbers of decision trees (ntree). At ntree = 100, the model achieved an R^2 of 0.663, with a concordance R^2 of 0.532. Increasing ntree to 200 resulted in a slight decrease in R^2 to 0.661, while the concordance R^2 remained stable at 0.533.

For ntree = 500, the model's R^2 improved again to 0.663, with a concordance R^2 of 0.534. However, at ntree = 1000, the R^2 slightly decreased to 0.661, with the concordance R^2 remaining at 0.533. These results indicate that while ntree influences model performance, the improvements plateau beyond 500 trees, suggesting limited additional benefits from further increasing decision trees. Figure 5 illustrates the concordance between actual and estimated AGB for different ntree values using vegetation indices.

Random forest regression model using both spectral bands and vegetation indices

The Random Forest (RF) regression model's performance in estimating Above Ground Biomass (AGB) was further analyzed using a combination of spectral bands and vegetation indices. At ntree = 100, the model achieved an R^2 of 0.675, with a concordance R^2 of 0.597. However, as ntree increased to 200, the R^2 slightly decreased to 0.668, while the concordance R^2 dropped to 0.580.

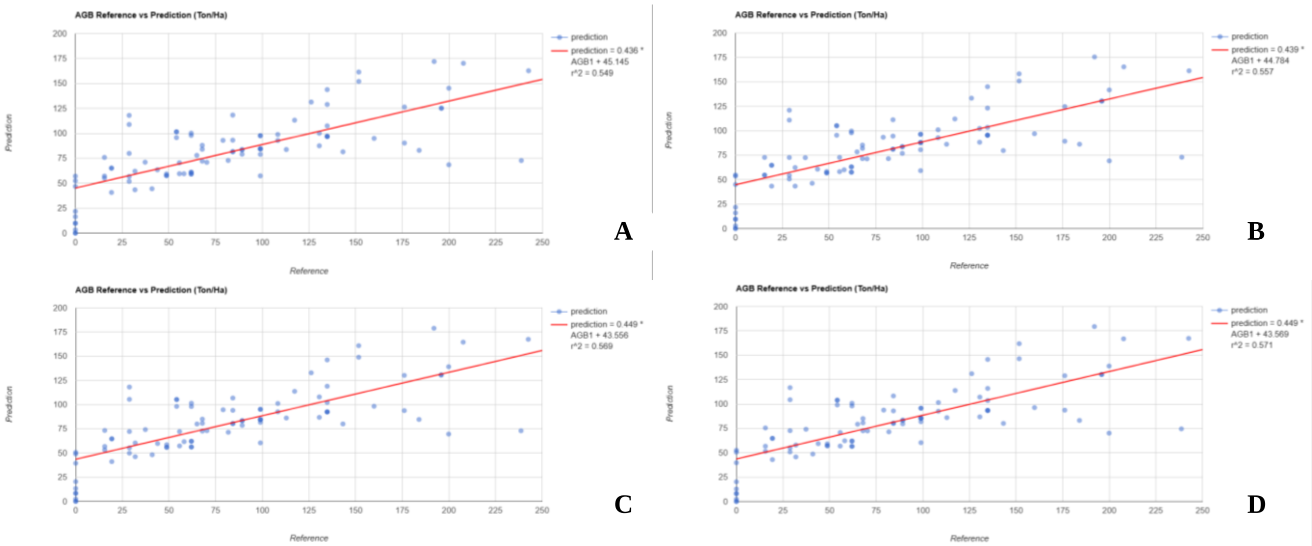

Figure 4. Correlation of actual AGB and estimates using spectral bands with different ntree: A. ntree = 100; B. ntree = 200; C. ntree = 500; D. ntree = 1000

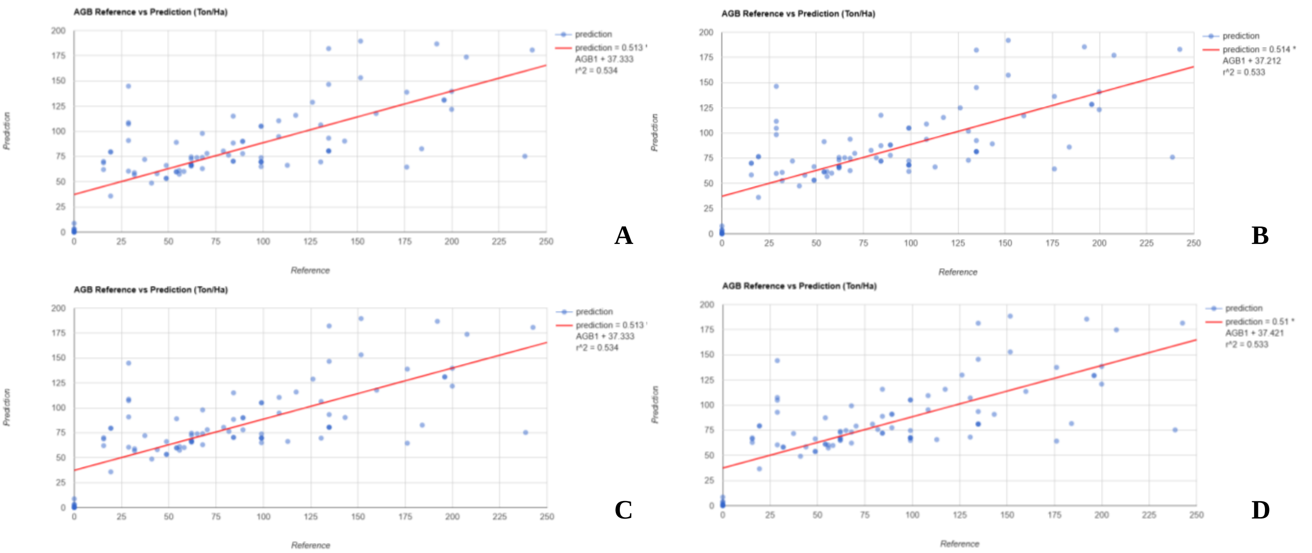

Figure 5. Correlation of actual AGB and estimates using VIs with different ntree: A. ntree = 100; B. ntree = 200; C. ntree = 500; D. ntree = 1000

Increasing ntree to 500 resulted in an R^2 of 0.670, with a concordance R^2 of 0.584. For ntree = 1000, the model's R^2 marginally improved to 0.671, with a concordance R^2 of 0.586. These results suggest that integrating both spectral bands and vegetation indices enhances the model's predictive performance compared to using either dataset alone. However, the improvements stabilize at higher ntree values, indicating diminishing returns beyond 500 trees. Figure 6 illustrates the concordance between actual and estimated AGB for different ntree values.

Estimating AGB map

Figure 7 illustrates the distribution of the estimated AGB values derived from the combination of spectral bands and vegetation indices for Dak Lak Province.

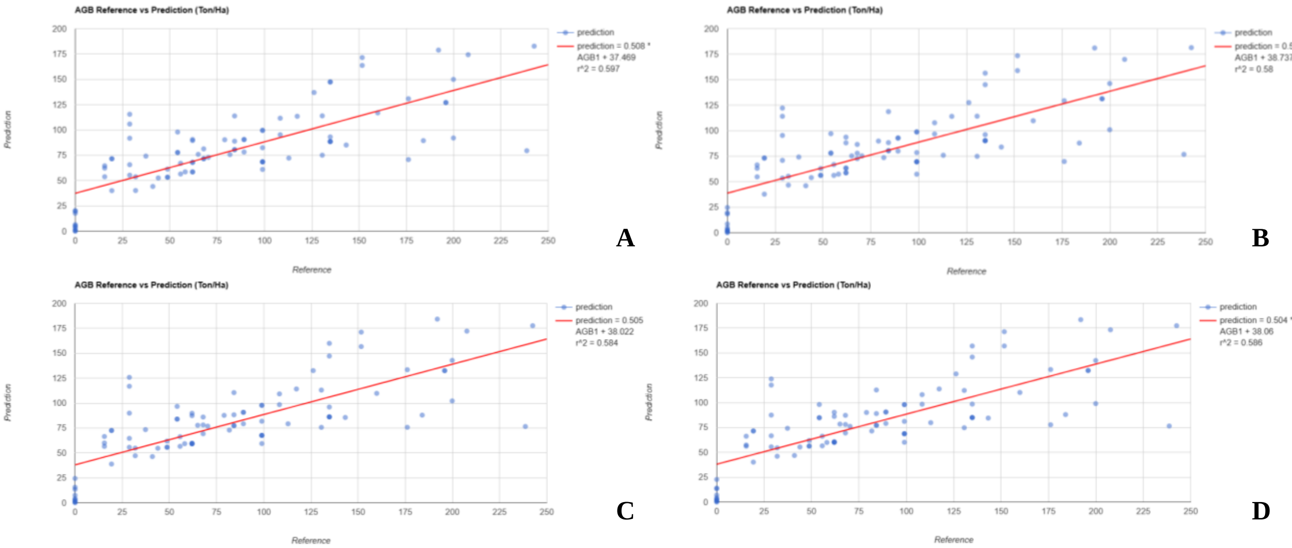

Figure 6. Correlation of actual AGB and estimates using VIs with different ntree: A. ntree = 100, B. ntree = 200, C. ntree = 500, and D. ntree = 1000

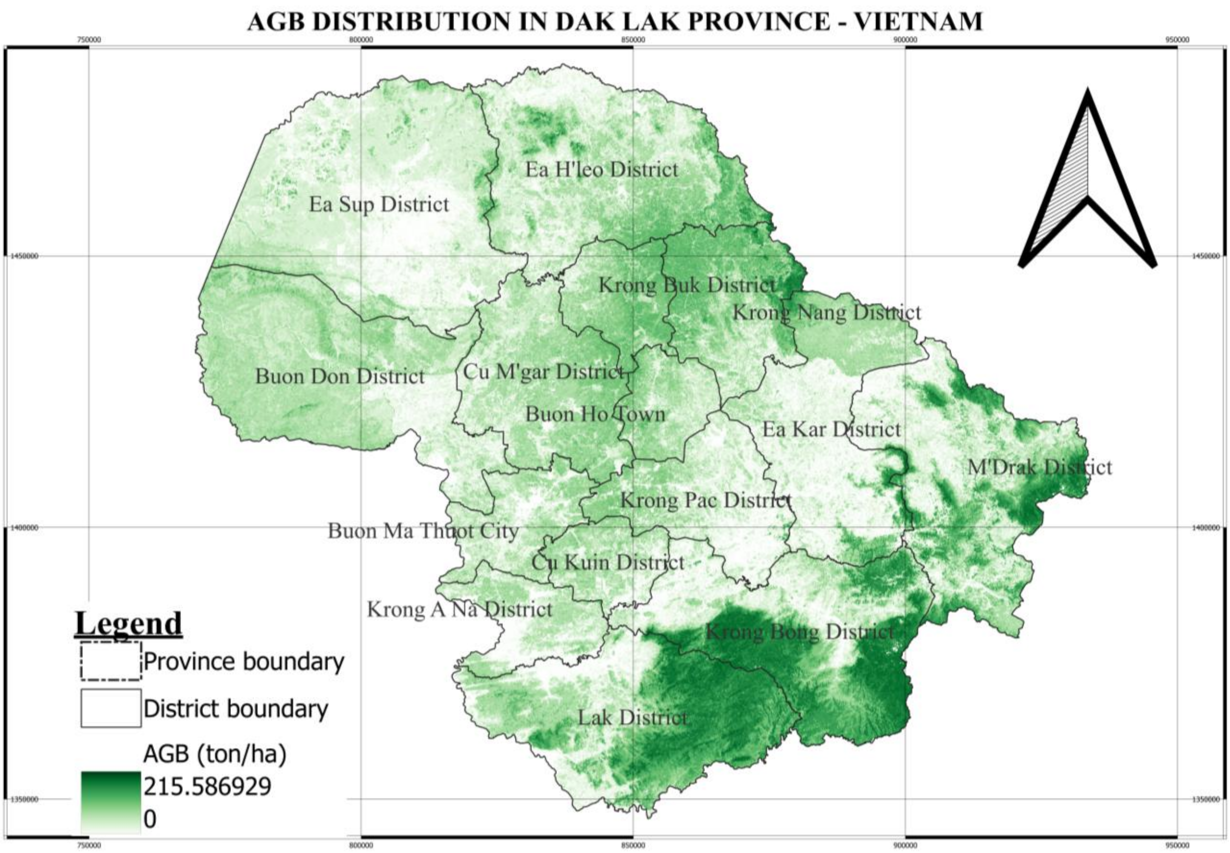

Figure 7. Estimated AGB value from the RF model in Dak Lak Province, Vietnam

The areas with the highest AGB storage in forests are predominantly located in the southern and eastern parts of the province, specifically in the districts of Lak, Krong Bong, M'Drak, and Ea Kar. These districts contain extensive natural broadleaf evergreen forests, which contribute significantly to their high biomass storage compared to other regions in the province.

Discussion

This study assessed the relationship between Above Ground Biomass (AGB) and Landsat 8 spectral bands, vegetation indices, and their combined application in predictive modeling. The findings provide significant insights into the performance of multiple linear regression and random forest regression models, as well as the spatial distribution of AGB across Dak Lak Province.

The multiple linear regression model identified a significant negative correlation between AGB and Band 6 ($p = 0.003$). However, its explanatory power was low ($R^2 = 0.131$), indicating that spectral bands alone may not sufficiently capture AGB variability. The nonsignificant contributions of Bands 4, 5, and 7 further suggest the necessity of incorporating additional variables, such as vegetation indices or environmental factors, to enhance prediction accuracy.

The random forest regression model outperformed the linear regression model, highlighting the efficacy of machine learning techniques in AGB estimation. Model accuracy improved with an increasing number of decision trees (ntree), with R^2 rising from 0.647 (ntree = 100) to 0.653 (ntree = 1000). Similarly, concordance between estimated and actual AGB consistently improved, plateauing at $R^2 = 0.571$ for ntree = 1000. These results indicate that while spectral data are valuable, their predictive capacity is limited when used in isolation.

The inclusion of vegetation indices further enhanced the model's predictive performance, reflecting their strong association with vegetation structure and biomass. The R^2 values ranged from 0.663 (ntree = 100) to 0.661 (ntree = 1000), while concordance between estimated and actual AGB exhibited slight improvement, stabilizing at $R^2 = 0.534$. Despite these gains, the marginal benefits observed with increasing ntree suggest a saturation point in the explanatory power of vegetation indices. The combination of spectral bands and vegetation indices yielded the most accurate AGB predictions, with R^2 values ranging from 0.675 (ntree = 100) to 0.671 (ntree = 1000), and concordance R^2 stabilizing at 0.586 for ntree = 1000. These findings emphasize the complementary nature of spectral and index-based data in capturing vegetation and forest structure characteristics. However, diminishing returns beyond ntree = 500 suggest an optimal tree number for balancing computational efficiency and model performance.

The spatial distribution of AGB, as estimated by the RF model, revealed distinct biomass variations across different forest types in Dak Lak Province. Evergreen broadleaf forests exhibited the highest AGB values, reflecting their dense vegetation structure and substantial carbon storage potential. In contrast, semi-evergreen and dry forests had lower AGB values, aligning with their less dense canopy cover and reduced biomass storage capacity.

The RF model demonstrated improved accuracy compared to previous studies in the Central Highlands. For instance, Bao et al. (2012) reported an R^2 of 0.53 when using only spectral bands, consistent with the lower predictive power observed in this study when relying solely on Landsat data (concordance $R^2 = 0.571$ for ntree = 1000). In contrast, combining spectral bands and vegetation indices in the present study enhanced RF model accuracy, achieving an R^2 of 0.671 and a concordance R^2 of 0.586 for ntree = 1000. These results reinforce the advantages of integrating vegetation indices, which capture additional information on vegetation structure and health, with spectral data for AGB estimation.

Moreover, these findings align with those of Dang et al. (2019), who reported an R^2 of 0.81 and RMSE of 36.67 Mg/ha using an RF model with combined spectral bands in dry dipterocarp forests. Although the R^2 achieved in this study was slightly lower, the results validate the applicability of RF algorithms for biomass estimation and demonstrate their effectiveness in capturing the spatial variability of AGB across diverse forest types. The spatial distribution analysis indicated high AGB concentrations in the southern and eastern districts, particularly in Lak, Krong Bong, M'Drak, and Ea Kar, where extensive broadleaf evergreen forests serve as significant carbon sinks. These results are consistent with previous studies highlighting the role of natural forest cover in biomass storage and climate change mitigation.

This study highlights the importance of integrating spectral data and vegetation indices for accurate AGB estimation. The superior performance of the RF model highlights the potential of machine learning approaches in modeling complex variable relationships. However, limitations include reliance on Landsat 8 data, which has moderate spatial resolution, and the exclusion of additional environmental variables, such as topography, soil characteristics, and climate data, that may influence AGB distribution. Future research should incorporate higher-resolution satellite imagery, such as Sentinel-2 or UAV-derived data, to improve spatial accuracy. Additionally, integrating environmental variables and testing alternative machine learning algorithms, such as gradient boosting or support vector regression, may further enhance AGB predictions. Expanding the study to other provinces with diverse forest types could also validate the model's applicability and generalizability.

In conclusion, this study evaluated the potential of random forest regression models in estimating aboveground biomass in Dak Lak Province, Vietnam, using Landsat 8 spectral bands, vegetation indices, and their combination. The results demonstrated that integrating spectral bands with vegetation indices yielded the most accurate AGB predictions, achieving an R^2 of 0.671 and a concordance R^2 of 0.586 with 1000 decision trees. These findings highlight the complementary role of spectral and index-based data in capturing vegetation structure and biomass. The spatial analysis indicated that evergreen broadleaf forests in the southern and eastern districts, including Lak, Krong Bong, M'Drak, and Ea Kar, had the highest AGB values. These forests serve as crucial carbon sinks, emphasizing their ecological significance and the necessity for conservation efforts. The RF model demonstrated superior performance compared to traditional linear regression and improved upon previous studies relying solely on spectral data. However, further accuracy improvements could be achieved by incorporating additional variables such as topography, soil properties, and climate factors, as well as utilizing higher-resolution satellite imagery. This study highlights the effectiveness of RF regression models in AGB estimation, offering a robust framework for forest biomass monitoring. These findings support sustainable forest management and climate change mitigation strategies in the Central Highlands Region of Vietnam.

ACKNOWLEDGEMENTS

We extend our deepest gratitude to the Ministry of Education and Training, Vietnam, for their invaluable support and funding, provided through project B2023-TTN-04, which laid the foundation for this research. Our sincere appreciation also goes to Tay Nguyen University for providing institutional support throughout the study. Additionally, we are grateful to the participants and stakeholders who generously contributed their time and insights, playing a crucial role in the data collection process. Lastly, we acknowledge the efforts of all individuals who, directly or indirectly, contributed to the successful completion of this work.

REFERENCES

Bao H, Vo H, Cao TL, Nguyen DD, Nguyen TTH, Pham DPQ, Nguyen CTA, Ho DB, Hoang TK. 2012. Determination of CO_2 sequestration of evergreen broadleaves forest in the Central Highlands of Vietnam as a basis for participation in the program of reducing emissions from deforestation and degradation. Final report, B2012-15-33TB, Daklak, Vietnam. Available at: http://baohuy-frem.org/vn/wp-content/uploads/sites/3/2016/07/B%C3%A1o-c%C3%A1o-%C4%91%E1%BB%81-t%C3%A0i-X%C3%A1c-%C4%91%E1%BB%8Bnh-CO2-h%E1%BA%A5p-th%E1%BB%A5-r%E1%BB%ABng-th%C6%B0%E1%BB%9Dng-xanh-T%C3%A2y-Nguy%C3%AAn.pdf.

Belgiu M, Drăguţ L. 2016. Random forest in remote sensing: A review of applications and future directions. ISPRS J Photogramm Remote Sens 114: 24-31. DOI: 10.1016/j.isprsjprs.2016.01.011.

Blackard JA, Finco MV, Helmer EH, Holden GR, Hoppus ML, Jacobs DM, Lister AJ, Moisen GG, Nelson MD, Riemann R, Ruefenacht B, Salajanu D, Weyermann DL, Winterberger KC, Brandeis TJ, Czaplewski RL, McRoberts RE, Patterson PL, Tymcio RP. 2008. Mapping U.S. forest biomass using nationwide forest inventory data and moderate resolution information. Remote Sens Environ 112 (4): 1658-1677. DOI: 10.1016/j.rse.2007.08.021.

Camarretta N, Jayathunga S, Wakelin SJ, Strand T, Dickinson Y. 2023. Maximising Forest Carbon: Review of Methods for Measuring Forest Carbon for National- and Property-Scale Reporting. Discussion Paper No: 2023/05, Ministry for Primary Industries Te Uru Rākau – New Zealand Forest Service. Available at: https://www.mpi.govt.nz/resources-and-forms/publications/.

Cao L, Coops NC, Innes JL, Sheppard SRJ, Fu L, Ruan H, She G. 2016. Estimation of forest biomass dynamics in subtropical forests using multi-temporal airborne LiDAR data. Remote Sens Environ 178: 158-171. DOI: 10.1016/j.rse.2016.03.012.

Carreiras JMB, Vasconcelos MJ, Lucas RM. 2012. Understanding the relationship between aboveground biomass and ALOS PALSAR data in the forests of Guinea-Bissau (West Africa). Remote Sens Environ 121: 426-442. DOI: 10.1016/j.rse.2012.02.012.

Dang ATN, Nandy S, Srinet R, Luong NV, Ghosh S, Kumar AS. 2019. Forest aboveground biomass estimation using machine learning regression algorithm in Yok Don National Park, Vietnam. Ecol Inform 50: 24-32. DOI: 10.1016/j.ecoinf.2018.12.010.

Deng S, Katoh M, Guan Q, Yin N, Li M. 2014. Estimating forest aboveground biomass by combining ALOS PALSAR and WorldView-2 data: A case study at Purple Mountain National Park, Nanjing, China. Remote Sens 6 (9): 7878-7910. DOI: 10.3390/rs6097878.

Duchelle AE, Simonet G, Sunderlin WD, Wunder S. 2018. What is REDD+ achieving on the ground? Curr Opin Environ Sustain 32: 134-140. DOI: 10.1016/j.cosust.2018.07.001.

Freeman EA, Moisen GG, Coulston JW, Wilson BT. 2016. Random forests and stochastic gradient boosting for predicting tree canopy cover: Comparing tuning processes and model performance. Can J For Res 46: 323-339. DOI: 10.1139/cjfr-2014-0562.

Gao Y, Lu D, Li G, Wang G, Chen Q, Liu L, Li D. 2018. Comparative analysis of modeling algorithms for forest aboveground biomass estimation in a subtropical region. Remote Sens 10 (4): 627. DOI: 10.3390/rs10040627.

Hao G, Dong Z, Hu L, Ouyang Q, Pan J, Liu X, Yang G, Sun C. 2024. Biomass inversion of highway slope based on unmanned aerial vehicle remote sensing and deep learning. Forests 15 (9): 1564. DOI: 10.3390/f15091564.

Hu Y, Sun Z. 2022. Assessing the capacities of different remote sensors in estimating forest stock volume based on high precision sample plot positioning and random forest method. Nat Environ Pollut Technol 21 (3): 1113-1123. DOI: 10.46488/NEPT.2022.v21i03.016.

Li C, Li Y, Li M. 2019. Improving forest aboveground biomass estimation by incorporating crown density and using Landsat 8 OLI images of a subtropical forest in Western Hunan, China. Forests 10 (2): 104. DOI: 10.3390/f10020104.

Li W, Chen E, Li Z, Ke Y, Zhan W. 2015. Forest aboveground biomass estimation using polarization coherence tomography and PolSAR segmentation. Intl J Remote Sens 36 (2): 530-550. DOI: 10.1080/01431161.2014.999383.

Li Y, Li M, Li C, Liu Z. 2020. Forest aboveground biomass estimation using Landsat 8 and Sentinel-1A data with machine learning algorithms. Sci Rep 10 (1): 9952. DOI: 10.1038/s41598-020-67024-3.

Liu Z, Peng C, Work T, Candau JN, DesRochers A, Kneeshaw D. 2018. Application of machine-learning methods in forest ecology: Recent progress and future challenges. Environ Rev 26 (4): 339-350. DOI: 10.1139/er2018-0034.

NASA. 2024. Landsat 8 Operational Land Imager (OLI) – Overview and Specifications. Retrieved from https://landsat.gsfc.nasa.gov/landsat-8/.

Nguyen TH, Jones S, Soto-Berelov M, Haywood A, Hislop S. 2020. Landsat time-series for estimating forest aboveground biomass and its dynamics across space and time: A review. Remote Sens 12 (1): 98. DOI: 10.3390/rs12010098.

Ouchra H, Belangour A, Erraissi A. 2023. Machine learning algorithms for satellite image classification using Google Earth Engine and Landsat Satellite data: Morocco case study. IEEE Access 11: 71127-71142. DOI: 10.1109/ACCESS.2023.3293828.

Probst P, Boulesteix AL. 2018. To tune or not to tune the number of trees in random forest? J Mach Learn Res 18: 1-18. DOI: 10.48550/arXiv.1705.05654.

Sa R, Nie Y, Chumachenko S, Fan W. 2024. Biomass estimation and saturation value determination based on multi-source remote sensing data. Remote Sens 16 (12): 2250. DOI: 10.3390/rs16122250.

Shen W, Li M, Huang C, Wei A. 2016. Quantifying live aboveground biomass and forest disturbance of mountainous natural and plantation forests in Northern Guangdong, China, based on multi-temporal Landsat, PALSAR and field plot data. Remote Sens 8 (7): 595. DOI: 10.3390/rs8070595.

Tian L, Wu X, Tao Y, Li M, Qian C, Liao L, Fu W. 2023. Review of remote sensing-based methods for forest aboveground biomass estimation: Progress, challenges, and prospects. Forests 14 (6): 1086. DOI: 10.3390/f14061086.

Tian X, Li J, Zhang F, Zhang H, Jiang M. 2024. Forest aboveground biomass estimation using multisource remote sensing data and deep learning algorithms: A case study over Hangzhou area in China. Remote Sens 16 (6): 1074. DOI: 10.3390/rs16061074.

USGS. 2023. Landsat Mission [Internet]. [cited 2023 Dec 20]. Available from: https://www.usgs.gov/landsat-missions/.

Wang L, Zhou X, Zhu X, Dong Z, Guo W. 2016. Estimation of biomass in wheat using random forest regression algorithm and remote sensing data. Crop J 4 (3): 212-219. DOI: 10.1016/j.cj.2016.01.008.

Wang T, Zhang H, Lin H, Fang C. 2015. Textural-spectral feature-based species classification of mangroves in Mai Po Nature Reserve from Worldview-3 imagery. Remote Sens 8 (1): 24. DOI: 10.3390/rs8010024.

West PW. 2015. Tree and forest measurement. Springer-Verlag Berlin Heidelberg. Springer Cham. DOI: 10.1007/978-3-319-14708-6.

Xiao J, Chevallier F, Gomez C, Guanter L, Hicke JA, Huete AR, Ichii K, Ni W, Pang Y, Rahman AF, Sun G, Yuan W, Zhang L, Zhang X. 2019. Remote sensing of the terrestrial carbon cycle: A review of advances over 50 years. Remote Sens Environ 233: 111383. DOI: 10.1016/j.rse.2019.111383.

Yang L, Liang S, Zhang Y. 2020. A new method for generating a global forest aboveground biomass map from multiple high-level satellite products and ancillary information. IEEE J Selected Topics in Appl Earth Observations Remote Sens 13: 2587-2597. DOI: 10.1109/JSTARS.2020.2987951.

Zhang L, Shao Z, Liu J, Cheng Q. 2019. Deep learning-based retrieval of forest aboveground biomass from combined LiDAR and Landsat 8 data. Remote Sens 11 (12): 1459. DOI: 10.3390/rs11121459.

Zhao K, Suarez JC, Garcia M, Hu T, Wang C, Londo A. 2018. Utility of multitemporal LiDAR for forest and carbon monitoring: Tree growth, biomass dynamics, and carbon flux. Remote Sens Environ 204: 883-897. DOI: 10.1016/j.rse.2017.09.007.